Overcoming Surfactant-Induced Morphology Instability of Noncrosslinked Diblock Copolymer Nano-objects Obtained by RAFT Emulsion Polymerization

Nghia P. Truong,[a] Cheng Zhang,[b,c] Tuan A.H. Nguyen,[d] Athina Anastasaki,[e] Morgan W. Schulze,[e] John F. Quinn,[a] Andrew K. Whittaker,[b,c] Craig J. Hawker,[e] Michael R. Whittaker*[a] and Thomas P. Davis*[a,f]

[a] ARC Centre of Excellence in Convergent Bio-Nano Science & Technology, Monash Institute of Pharmaceutical Sciences, Monash University, Melbourne, Victoria 3052, Australia.

[b] Australian Institute for Bioengineering and Nanotechnology, [c]ARC Centre of Excellence in Convergent Bio-Nano Science & Technology, and [d]School of Chemical Engineering, The University of Queensland, Brisbane, Qld 4072, Australia.

[e] Materials Research Laboratory, University of California, Santa Barbara, California 93106, USA

[f] Department of Chemistry, University of Warwick, Coventry CV4 7AL, United Kingdom.

ABSTRACT: RAFT emulsion polymerization techniques including polymerization-induced self-assembly (PISA) and temperature-induced morphological transformation (TIMT) are widely used to produce noncrosslinked nano-objects with various morphologies. However, the worm, vesicle and lamellar morphologies produced by these techniques typically cannot tolerate the presence of added surfactants, thus limiting their potential applications. Herein we report the surfactant tolerance of noncrosslinked worms, vesicles and lamellae prepared by RAFT emulsion polymerizations using poly(di(ethylene glycol) ethyl ether methacrylate-*co*-*N*-(2-hydroxypropyl) methacrylamide) (P(DEGMA-*co*-HPMA)) as a macromolecular chain transfer agent (macro-CTA). Significantly, these P(DEGMA-*co*-HPMA) nanoparticles are highly stable in concentrated solutions of surfactants (e.g., sodium dodecyl sulfate (SDS)). We also demonstrate that the surfactant tolerance is related to the limited binding of SDS to the main-chain of the P(DEGMA-*co*-HPMA) macro-CTA constituting the particle shell. This work provides new insight into the interactions between surfactants and thermoresponsive copolymers, and expands the scope of RAFT emulsion polymerization techniques for the preparation of noncrosslinked and surfactant-tolerant nanomaterials.

The morphology of polymeric nanomaterials has been identified as a crucial factor that impacts their properties and applications.[1-2] Elongated shape is beneficial to building blocks for three-dimensional superstructures, templates for catalysis, and extracellular matrices for tissue engineering.[3-4] In nanomedicine, morphology affects various biological parameters including circulation time, biodistribution, cellular uptake and efficiency of nanocarriers.[5-7] The synthesis of nanomaterials with stable morphologies is therefore critical and has attracted increasing attention.[8]

Reversible addition fragmentation chain transfer (RAFT) emulsion polymerization techniques including polymerization-induced self-assembly (PISA) and temperature-induced morphological transformation (TIMT) have been recognized as simple, rapid, and environmentally friendly methods for the scalable synthesis of polymeric nano-objects with different morphologies.[9-10] In PISA, water-soluble macromolecular chain transfer agents (macro-CTAs) are copolymerized with water-insoluble monomers to form *in-situ* core-shell micelles of tunable size and shape.[11-14] In TIMT, thermoresponsive rather than water-soluble macro-CTAs are employed (e.g., thermoresponsive poly((di(ethylene glycol) methyl ether methacrylate)-*co*-*N*-(2-hydroxypropyl) methacrylamide) (P(DEGMA-*co*-HPMA)).[15-16] Nanomaterials produced by these techniques have been used for diverse applications.[17-18]

Notwithstanding the advantages outlined above, the current limitation of the RAFT emulsion polymerization is that the morphologies of noncrosslinked diblock copolymer nanoparticles typically are not stable in a concentrated solution of surfactant.[19] The addition of anionic surfactant to suspensions of nano-objects prepared by PISA leads to the rapid dissociation of these nanomaterials to molecularly dissolved copolymer chains.[20] In addition, worm, vesicle and lamellar morphologies prepared by TIMT were all transformed to a spherical shape when sodium dodecyl sulfate (SDS) was added.[21] The destruction and morphological instability of

these nano-objects are attributed to the increased solubility of polymer chains or the decrease in the critical packing parameter (p) of the nano-objects due to the binding of SDS to the macro-CTAs constituting the nanoparticle shell.[20-22] This drawback critically limits the potential applications of these synthetic techniques, particularly for home and personal care products.[19]

Considerable efforts have been made to overcome the surfactant-induced instability of these nanoparticle morphologies by covalently crosslinking the nano-objects.[23-24] For example, Armes and co-workers have developed a postmodification technique using epoxy-amine chemistry to crosslink the hydrophilic domain of the vesicle membrane.[20] An and colleagues used an asymmetric crosslinker bearing two vinyl groups of different reactivities to *in-situ* crosslink the hydrophobic part of the vesicle membrane.[25-27] The use of crosslinkers is likely to increase colloidal instability, is less reliable for worm morphology, and more importantly, is not applicable for stimuli-responsive nanomaterials.[19] These inherent disadvantages require urgent alternative solutions.[28]

A potential approach to overcome this surfactant induced morphology instability without the use of crosslinkers is to employ macro-CTAs that have limited binding with surfactants. In nanomedicine, poly(ethylene glycol) (PEG) and PHPMA are widely used as antifouling polymers to reduce the binding of surfactant-like molecules (e.g., proteins).[29-30] However, to date there has been no comprehensive study on the binding of surfactants to ethylene glycol- and PHPMA-based thermoresponsive copolymers such as P(DEGMA-*co*-HPMA). In addition, it remains unclear whether noncrosslinked nanoparticles having P(DEGMA-*co*-HPMA) as the corona are stable in the presence of added surfactants.

To address this challenge, we studied the surfactant tolerance of nano-objects prepared by RAFT emulsion polymerization using P(DEGMA-*co*-HPMA) as the macro-CTA and investigated interactions between this thermoresponsive polymer and SDS. Firstly, nanoparticles having worm, vesicle and lamellar morphologies were synthesized by RAFT emulsion polymerization. The morphologies and the surfactant tolerance of these nanoparticles were characterized by transmission electron microscopy (TEM) and small angle X-ray scattering (SAXS). Next, the interaction between P(DEGMA-*co*-HPMA) macro-CTA and SDS was investigated using molecular dynamics (MD) simulation and nuclear Overhauser effect spectroscopy (NOESY). Finally, pulsed-field gradient NMR (PFG-NMR) was employed to estimate the mole fraction of SDS bound to the macro-CTA.

To prepare nano-objects with various morphologies (Scheme 1), RAFT emulsion polymerizations using the P($DEGMA_{29}$-*co*-$HPMA_6$) macro-CTA were carried out as previously described.[31] The hot suspension obtained after polymerization was cooled to ambient temperature (T < cloud point temperature (T_{cp})) in the presence of appropriate amounts of added plasticizer (toluene for polystyrene (PS), propyl methacrylate (PMA) for PPMA).[32]

Scheme 1. (A) Synthesis of worms, vesicles and lamellae via RAFT emulsion polymerization of styrene and (B) representative cartoons for temperature-induced morphological transformation.

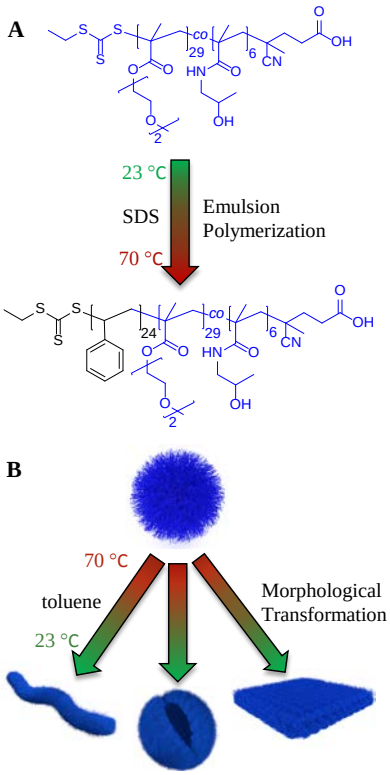

During cooling, the thermoresponsive block of the diblock copolymer (~19 mg mL^{-1}) transitioned from water-insoluble to water-soluble, which induced the reorganization of the diblock copolymer chains and the transformation of the initially self-assembled spheres to other morphologies (worm, vesicle, or lamellae).[15]

The cloudy suspensions were obtained (denoted as latexes) and characterized by TEM. Figure 1A-C showed worm, a mixture of worm and vesicle, and lamellar morphologies when different concentrations of plasticizer were added (40 µL mL^{-1}, 80 µL mL^{-1}, and 160 µL mL^{-1}, respectively). This result is consistent with our previous observations, thus highlighting the reproducibility of the TIMT technique.[31] To identify if there is a small decrease in the p value upon adding SDS, we synthesized a mixture of worms and vesicles (p ~ 1/2) but not pure vesicles (1 > p > 1/2) because a small decrease in the p value of pure vesicles (e.g., from p ~ 0.7 to p ~ 0.6) is not expected to result in the loss of this morphology. In addition to using plasticizer, the morphology of the nanoparticles prepared by TIMT has been also controlled via manipulating the molecular weight of the thermoresponsive and/or the water-insoluble block.[31] However, changing the molecular weight of diblock copolymers has been found to affect the stability of their nanoparticles (e.g., aggregation or dissolution).[33-34] As such, we have chosen to tune the nanoparticle shape by using plasticizers in order to decouple polymer molecular weight from particle stability.

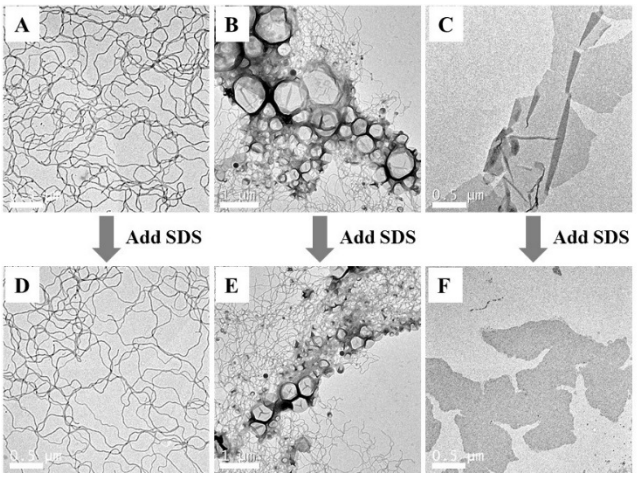

Figure 1. Upper row shows representative TEM images of the polystyrene latexes after emulsion polymerization and addition of (A) 40 μL mL^{-1}, (B) 80 μL mL^{-1}, (C) 160 μL mL^{-1} of toluene, followed by cooling to room temperature for 24 h. Bottom row shows representative TEM images of latexes (D), (E), (F) obtained by adding SDS (5 mg) to latexes (A), (B), (C) (0.5 mL), respectively. Scale bars for (B) and (E) were 1 μm. Other scale bars represent 0.5 μm.

Next, SDS (5 mg) was added to the latexes of worms, mixed worms and vesicles, and lamellae (0.5 mL), vortexed for 1 min, and subsequently characterized by TEM. Interestingly, Figure 1D-F showed that morphologies of all nano-objects made from the P(DEGMA$_{29}$-*co*-HPMA$_6$) macro-CTA were stable in concentrated SDS solution (up to 10 mg mL^{-1}). To complement these TEM images, SAXS was used to analyze the worm morphology in solution with and without adding SDS by fitting the scattering profiles to a theoretical model for cylindrical objects.[35] In Figure 2A, the scattering profile of the worm latex was satisfactorily fit using a cylindrical model (black solid line) suggesting that the majority of nanoparticles in solution had worm-like morphology.[36] Importantly, the scattering profile of the worm latex upon the addition of SDS (Figure 2B) revealed a similar pattern in agreement with the cylindrical model, thus confirming that the P(DEGMA$_{29}$-*co*-HPMA$_6$) nanoparticles were stable in the presence of added SDS. Significantly, the worm latex was also highly stable in the presence of alternative surfactants such as cationic decyltrimethylammonium bromide (Figure S1). These results illustrate the robust and stable nature of polymeric nanostructures based on P(DEGMA$_{29}$-*co*-HPMA$_6$) in concentrated surfactant solutions.

The surfactant tolerance identified in this work is in stark contrast to the surfactant-induced dissociation or morphological transformation found for the majority of noncrosslinked nano-objects previously prepared by PISA and TIMT.[19] For example, worms, vesicles, and lamellae comprising a similar PS core but a thermoresponsive poly(*N*-isopropylacrylmide)(PNIPAM) shell have been found to transform into spheres when SDS was added.[21] This transformation is related to a decrease in the critical packing parameter (*p*).[21] Particularly, on adding SDS to the latexes of PS-b-PNIPAM nanoparticles, the added SDS

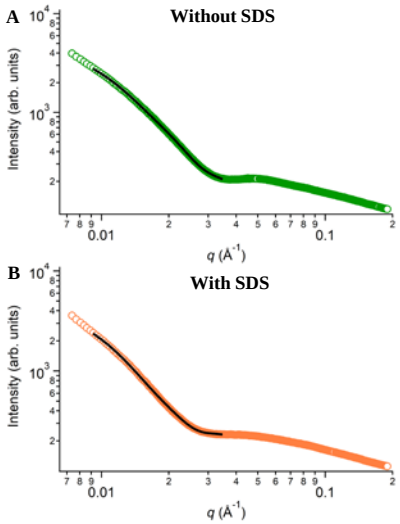

Figure 2. SAXS patterns for the worm latex (A) before and (B) after the addition of SDS (10 mg mL^{-1}) at ambient temperature. The black solid line is theoretical fitting of experimental data to a cylindrical model using SASview software.

molecules bind to the PNIPAM side chains of the particle surface.[21] This binding increases the effective interfacial area at the hydrophobic-water interface (*a*) such that the packing parameter decreases to a value consistent with a spherical morphology ($p < 1/3$), as given by eq 1:[37]

$$p = v / al \quad (1)$$

where *p* is the critical packing parameter; *v* is the volume of hydrophobic chains; *a* is an effective interfacial area at the hydrophobic-water interface; and *l* is the length of hydrophobic chains.

In contrast, the packing parameter of P(DEGMA$_{29}$-*co*-HPMA$_6$) nanoparticles exhibited no significant change upon the addition of SDS as demonstrated by the high stability of worms, lamellae and the mixture of worms and vesicles. As detailed above, even a small decrease in the *p* value upon adding SDS to the latex of worms and vesicles (from $p \sim 1/2$ for worms and vesicles to $p < 1/2$ for worms only) typically results in the disappearance of the vesicle morphology. However, the vesicle morphology was clearly observed in Figure 1E suggesting that the *p* value was unchanged. Further, the plasticizer (toluene) remained inside the swollen PS cores so the morphologies of these nano-objects were not kinetically frozen due to the glassy PS core ($T_{g,PS}$ = 95 °C).[16] Similarly, nano-objects with a P(DEGMA$_{29}$-*co*-HPMA$_6$) shell and less glassy PPMA core ($T_{g,PPMA}$ = 31 °C)[16] were also tolerant to added SDS (Figure S2). Based on these observations, we hypothesize that added SDS has limited binding to P(DEGMA$_{29}$-*co*-HPMA$_6$) domains so that the packing parameter remains unchanged upon adding SDS. While the interactions between SDS and thermoresponsive PNIPAM have been well-documented in the literature,[38] the binding of surfactants to ethylene glycol- and PHPMA-based thermoresponsive copolymers has not been investigated.

To study the molecular interaction between SDS and P(DEGMA$_{29}$-*co*-HPMA$_6$) at ambient temperature, 2D

NOESY NMR was initially employed. The mixing time and other parameters used for NOESY NMR were carefully chosen.[39-41] In Figure 3A, strong positive cross-relaxation peaks between representative alkyl protons for the SDS surfactant (peak *g*) and those of the P(DEGMA$_{29}$-*co*-HPMA$_6$) domains are clearly observed. This observation suggested that at ambient temperature, SDS molecules associated closely to P(DEGMA$_{29}$-*co*-HPMA$_6$) chains, typically over distances smaller than 0.5 nm.[42] This association is similar to the binding of SDS to PNIPAM at ambient temperature reported by Chen *et. al*.[38] While the association is similar, the binding sites of SDS to the P(DEGMA$_{29}$-*co*-HPMA$_6$) chains is distinctly different to that observed for PNIPAM. As shown in Figure 3B, the normalized cross-peak intensity between the alkyl protons of SDS (peak *g*) and the protons of P(DEGMA$_{29}$-*co*-HPMA$_6$) backbone (peak *h*) is significantly higher than for the P(DEGMA$_{29}$-*co*-HPMA$_6$) side chains (peaks *a-f*) indicating that SDS associates primarily with the backbone of P(DEGMA$_{29}$-*co*-HPMA$_6$) chains. In contrast, SDS associates strongly with the isopropyl group of the PNIPAM side chain.[38] These NOESY NMR studies provide a useful molecular-level understanding of the interactions between SDS and P(DEGMA$_{29}$-*co*-HPMA$_6$) at ambient temperature.

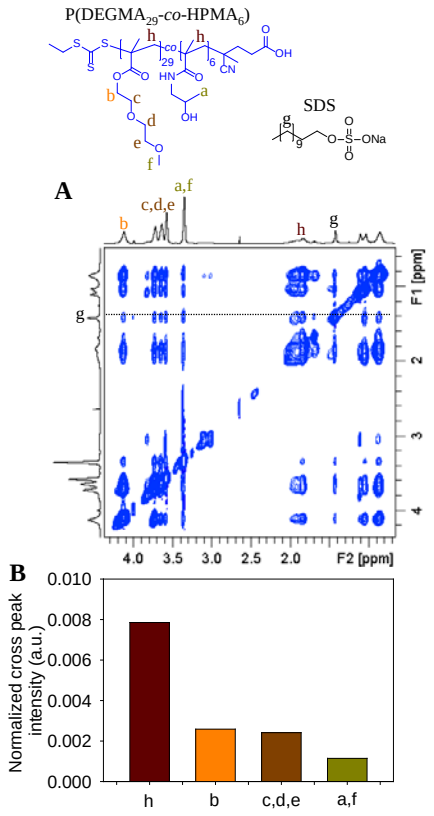

Figure 3. (A) ^{1}H – ^{1}H 2D NOESY spectrum of P(DEGMA$_{29}$-*co*-HPMA$_6$)/SDS/D$_2$O solution (12.5 mg/0.25 mg/1 mL). (B) Normalized cross-peak intensities at ambient temperature of protons *g* to protons of P(DEGMA$_{29}$-*co*-HPMA$_6$). These values were calculated from the NOESY spectrum by using the diagonal cross-peaks generated from the methylene protons from SDS.

To further understand the interaction between SDS and P(DEGMA$_{29}$-*co*-HPMA$_6$), ^{1}H NOESY experiments were conducted at a series of elevated temperatures with the results being supported by MD simulations. At temperatures above the T_{cp}, the association of SDS molecules with the P(DEGMA$_{29}$-*co*-HPMA$_6$) backbone decreases, which is similar to the behavior observed between SDS and PNIPAM at higher temperatures.[38] In particular, Figure 4A showed a decrease in normalized cross-peak intensities between the protons *g* and those of P(DEGMA$_{29}$-*co*-HPMA$_6$) indicating the dissociation of SDS/P(DEGMA$_{29}$-*co*-HPMA$_6$) as the solution temperature increased. The dissociation observed by NOESY NMR is in close agreement with the data obtained by MD simulation indicating that the distance between protons *g* of SDS and protons *h* of the P(DEGMA$_{29}$-*co*-HPMA$_6$) backbone increased at higher temperature (Figure 4B). Taken together, both NOESY NMR and MD simulation results suggest that the binding between SDS and P(DEGMA$_{29}$-*co*-HPMA$_6$) is dynamic and sensitive to increasing temperature. However, the stabilization of P(DEGMA$_{29}$-*co*-HPMA$_6$) particles formed at 70 °C during emulsion polymerization indicates that a fraction of the SDS molecules remains associated with the P(DEGMA$_{29}$-*co*-HPMA$_6$) domains of the nanoparticles.

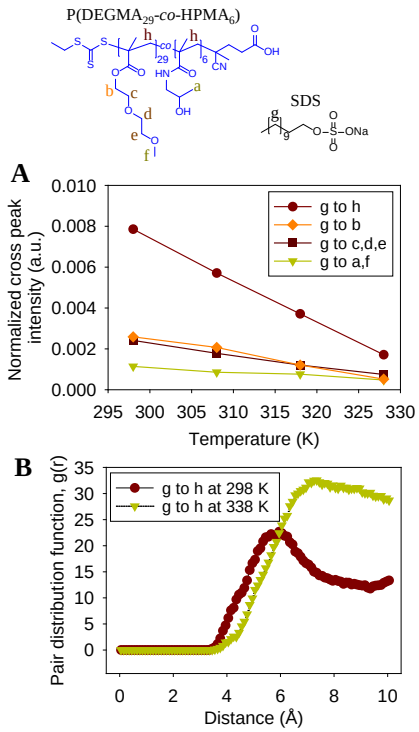

Figure 4. (A) Normalized cross-peak intensities at different temperatures. (B) Pair distribution function vs. distance between protons *g* of SDS and protons *h* of P(DEGMA$_{29}$-*co*-HPMA$_6$) at 298K and 338K.

To quantitatively estimate the mole fraction of SDS bound to P(DEGMA$_{29}$-*co*-HPMA$_6$) chains, self-diffusion coefficients (*D*) were determined using PFG-NMR (see the experimental for more details).[43-44] The quality of the fit of a single diffusion coefficient to the echo attenuation data

was extremely good (Figure S3). Moreover, the presence of a second component in the plots can be confidently excluded. Previously, Chen and coworkers have employed a similar strategy to determine the molar percentage of SDS molecules bound to PNIPAM chains under comparable conditions.[38] In this analysis, the mole fractions of SDS molecules bound to P(DEGMA$_{29}$-*co*-HPMA$_6$) chains (f_{bound}) at various temperatures and concentrations were calculated as using eq 2:[45]

$$D_{obs} = f_{free}.D_{free} + f_{bound}D_{bound} \quad (2)$$

where D_{obs} is the single, observed self-diffusion coefficient of SDS , f_{free} is the mole fraction of free SDS, D_{free} is the self-diffusion coefficient of SDS measured in a solution in the absence of the polymer, f_{bound} is the mole fraction of SDS bound to the polymer chains and D_{bound} is the self-diffusion coefficient of the bound SDS, assumed to be the same as the measured diffusion coefficient for the polymer.[45]

In Table 1, f_{bound} is shown to decrease when the solution temperature is higher than the T_{cp}. Significantly, a large number of SDS molecules are still associated with the P(DEGMA$_{29}$-*co*-HPMA$_6$) chains, even at temperatures well above the T_{cp}. This result is consistent with the partial dissociation of SDS/P(DEGMA$_{29}$-*co*-HPMA$_6$) at elevated temperature observed in the NOESY NMR results whilst the observation of bound SDS explains the stabilization of P(DEGMA$_{29}$-*co*-HPMA$_6$) particles formed at high temperature prior to and during the emulsion polymerization. Furthermore, at ambient temperature, f_{bound} also decreased at the SDS concentration of 10 mg ml^{-1} (well above the critical micellization concentration of SDS – 2.5 mg mL^{-1})[38] indicating that a large portion of added SDS molecules tended to form SDS aggregates (with alkyl groups as the core and sulfate groups as the shell) rather than co-assembly with P(DEGMA$_{29}$-*co*-HPMA$_6$) chains.[46] Altogether, the data obtained from the PFG-NMR supported our hypothesis that a limited amount of added SDS binds to P(DEGMA$_{29}$-*co*-HPMA$_6$) chains, thus leading to the surfactant tolerance of noncrosslinked nanoparticles made from P(DEGMA-*co*-HPMA) macro-CTA. Further, the nature of the binding between SDS and P(DEGMA-*co*-HPMA) is dynamic and sensitive to both temperature and SDS concentration.

Table 1. Diffusion coefficients (D) and mole fractions of SDS-bound polymer (f_{bound}).

T (K)	[SDS] (mg mL^{-1})	D x 10^{10} (m^2 s^{-1})			f_{bound}
		D_{free}	D_{obs}	D_{bound}	
298	0.25	7.53	1.67	1.48	1.0
308	0.25	10.4	0.95	0.81	1.0
318	0.25	12.5	3.93	2.45	0.9
328	0.25	15.7	6.45	3.34	0.8
298	1.25	7.41	1.54	1.43	1.0
298	2.50	6.53	1.64	1.40	1.0
298	10.0	1.95	1.53	1.12	0.5

In conclusion, we have demonstrated the enhanced stability in concentrated surfactant solutions and the morphological richness of noncrosslinked nano-objects prepared by RAFT emulsion polymerization using P(DEGMA$_{29}$-*co*-HPMA$_6$) as a macro-CTA. The combination of NOESY, PFG-NMR and MD simulations reveals that at low temperature and concentration, SDS molecules bind to the backbone of P(DEGMA$_{29}$-*co*-HPMA$_6$) with partial dissociation of this assembly occurring as elevated temperatures. A significant fraction of SDS remains bound at elevated temperatures providing colloidal stability to P(DEGMA$_{29}$-*co*-HPMA$_6$) particles formed at the beginning and during the emulsion polymerization process. These findings illustrate a distinct interaction between SDS and the thermoresponsive P(DEGMA$_{29}$-*co*-HPMA$_6$) chains as well as the mechanism of SDS-stabilized thermoresponsive nanoparticles. Significantly, the morphologies of the noncrosslinked P(DEGMA-*co*-HPMA) particles are not affected by the introduction of SDS at room temperature leading to the surfactant tolerance and increasing the applicability of noncrosslinked nano-objects prepared by RAFT emulsion polymerization techniques.

ASSOCIATED CONTENT

Supporting Information.
The Supporting Information is available free of charge on the ACS Publications website at DOI: 10.1021/acsmacrolett.7b00978.

Experimental details (**PDF**).

AUTHOR INFORMATION

Corresponding Author

* Email: michael.whittaker@monash.edu.
* Email: thomas.p.davis@monash.edu.

ACKNOWLEDGMENT

Electron microscopy was performed at the Bio21 Advanced Microscopy Facility, The University of Melbourne. SAXS experiments were performed at Beamline 1-5 of Stanford Synchrotron Radiation Lightsource (SSRL). Use of the SSRL, a Directorate of the SLAC National Accelerator Laboratory, is supported by the U.S. Department of Energy, Office of Science, Office of Basic Energy Sciences under Contract No. DE-AC02-76SF0051. This work benefited from the use of the SasView application, originally developed under NSF award DMR-0520547. SasView contains code developed with funding from the European Union's Horizon 2020 research and innovation programme under the SINE2020 project, grant agreement No. 654000.
This work was carried out within the Australian Research Council (ARC) Centre of Excellence in Convergent Bio-Nano Science and Technology (Project No. CE140100036). N.P.T. acknowledges the award of a DECRA Fellowship from the Australian Research Council (DE180100076). C.Z. acknowledges the University of Queensland for his Early Career Researcher Grant (UQECR1720289). T.A.H.N. acknowledges the University of Queensland for his Early Career Researcher Grant (UQECR1720169). A.A. is grateful to

the European Union (EU) for a Marie Curie Postdoctoral Fellowship and the California NanoSystems Institute for an Elings Prize Fellowship in Experimental Science. J.F.Q. acknowledges receipt of a Future Fellowship from the ARC (FT170100144). T.P.D. is grateful for the award of an Australian Laureate Fellowship from the ARC (FL140100052).

REFERENCES

1. Hinde, E.; Thammasiraphop, K.; Duong, H. T.; Yeow, J.; Karagoz, B.; Boyer, C.; Gooding, J. J.; Gaus, K., Pair correlation microscopy reveals the role of nanoparticle shape in intracellular transport and site of drug release. *Nat. Nanotechnol.* **2017,** *12* (1), 81-89.

2. Ta, H. T.; Truong, N. P.; Whittaker, A. K.; Davis, T. P.; Peter, K., The effects of particle size, shape, density and flow characteristics on particle margination to vascular walls in cardiovascular diseases. *Expert Opin. Drug Deliv.* **2017**, 33-45.

3. Truong, N. P.; Quinn, J. F.; Whittaker, M. R.; Davis, T. P., Polymeric filomicelles and nanoworms: two decades of synthesis and application. *Polym. Chem.* **2016,** *7* (26), 4295-4312.

4. Cheng, C.; Qi, K.; Germack, D. S.; Khoshdel, E.; Wooley, K. L., Synthesis of core-crosslinked nanoparticles with controlled cylindrical shape and narrowly-dispersed size via core-shell brush block copolymer templates. *Adv. Mater.* **2007,** *19* (19), 2830-+.

5. Truong, N. P.; Whittaker, M. R.; Mak, C. W.; Davis, T. P., The importance of nanoparticle shape in cancer drug delivery. *Expert Opin. Drug Deliv.* **2015,** *12* (1), 129-142.

6. Kaga, S.; Truong, N. P.; Esser, L.; Senyschyn, D.; Sanyal, A.; Sanyal, R.; Quinn, J. F.; Davis, T. P.; Kaminskas, L. M.; Whittaker, M. R., Influence of Size and Shape on the Biodistribution of Nanoparticles Prepared by Polymerization-Induced Self-Assembly (PISA). *Biomacromolecules* **2017,** *18* (12), 3963–3970.

7. Truong, N. P.; Gu, W. Y.; Prasadam, I.; Jia, Z. F.; Crawford, R.; Xiao, Y.; Monteiro, M. J., An influenza virus-inspired polymer system for the timed release of siRNA. *Nat. Commun.* **2013,** *4*, 1902.

8. Truong, N. P.; Quinn, J. F.; Dussert, M. V.; Sousa, N. B. T.; Whittaker, M. R.; Davis, T. P., Reproducible Access to Tunable Morphologies via the Self-Assembly of an Amphiphilic Diblock Copolymer in Water. *ACS Macro Letters* **2015,** *4*, 381-386.

9. Warren, N. J.; Armes, S. P., Polymerization-induced self-assembly of block copolymer nano-objects via RAFT aqueous dispersion polymerization. *J. Am. Chem. Soc.* **2014,** *136* (29), 10174-85.

10. Engelis, N. G.; Anastasaki, A.; Nurumbetov, G.; Truong, N. P.; Nikolaou, V.; Shegiwal, A.; Whittaker, M. R.; Davis, T. P.; Haddleton, D. M., Sequence-controlled methacrylic multiblock copolymers via sulfur-free RAFT emulsion polymerization. *Nat. Chem.* **2016**, 171-178.

11. Truong, N. P.; Dussert, M. V.; Whittaker, M. R.; Quinn, J. F.; Davis, T. P., Rapid synthesis of ultrahigh molecular weight and low polydispersity polystyrene diblock copolymers by RAFT-mediated emulsion polymerization. *Polym. Chem.* **2015,** *6*, 3865-3874.

12. Wang, X.; Figg, C. A.; Lv, X. Q.; Yang, Y. Q.; Sumerlin, B. S.; An, Z. S., Star Architecture Promoting Morphological Transitions during Polymerization-Induced Self-Assembly. *Acs Macro Letters* **2017,** *6* (4), 337-342.

13. Khor, S. Y.; Truong, N. P.; Quinn, J. F.; Whittaker, M. R.; Davis, T. P., Polymerization-Induced Self-Assembly: The Effect of End Group and Initiator Concentration on Morphology of Nanoparticles Prepared via RAFT Aqueous Emulsion Polymerization. *ACS Macro Letters* **2017,** *6* (9), 1013-1019.

14. Tan, J.; Sun, H.; Yu, M.; Sumerlin, B. S.; Zhang, L., Photo-PISA: Shedding Light on Polymerization-Induced Self-Assembly. *ACS Macro Letters* **2015,** *4* (11), 1249-1253.

15. Truong, N. P.; Quinn, J. F.; Anastasaki, A.; Rolland, M.; Vu, M.; Haddleton, D.; Whittaker, M. R.; Davis, T. P., Surfactant-free RAFT emulsion polymerization using a novel biocompatible thermoresponsive polymer. *Polym. Chem.* **2017**, 1353-1363.

16. Truong, N. P.; Quinn, J. F.; Anastasaki, A.; Haddleton, D. M.; Whittaker, M. R.; Davis, T. P., Facile access to thermoresponsive filomicelles with tuneable cores. *Chem. Commun.* **2016,** 52, 4497-4500.

17. Esser, L.; Truong, N. P.; Karagoz, B.; Moffat, B. A.; Boyer, C.; Quinn, J. F.; Whittaker, M. R.; Davis, T. P., Gadolinium-functionalized nanoparticles for application as magnetic resonance imaging contrast agents via polymerization-induced self-assembly. *Polym. Chem.* **2016,** *7* (47), 7325-7337.

18. Zhao, W.; Ta, H. T.; Zhang, C.; Whittaker, A. K., Polymerization-Induced Self-Assembly (PISA) - Control over the Morphology of F-19-Containing Polymeric Nano-objects for Cell Uptake and Tracking. *Biomacromolecules* **2017,** *18* (4), 1145-1156.

19. Canning, S. L.; Smith, G. N.; Armes, S. P., A Critical Appraisal of RAFT-Mediated Polymerization-Induced Self-Assembly. *Macromolecules* **2016,** *49* (6), 1985-2001.

20. Chambon, P.; Blanazs, A.; Battaglia, G.; Armes, S. P., How Does Cross-Linking Affect the Stability of Block Copolymer Vesicles in the Presence of Surfactant? *Langmuir* **2012,** *28* (2), 1196-1205.

21. Jia, Z. F.; Truong, N. P.; Monteiro, M. J., Reversible polymer nanostructures by regulating SDS/PNIPAM binding. *Polym. Chem.* **2013,** *4* (2), 233-236.

22. Rufier, C.; Collet, A.; Viguier, M.; Oberdisse, J.; Mora, S., SDS Interactions with Hydrophobically End-Capped Poly(ethylene oxide) Studied by C-13 NMR and SANS. *Macromolecules* **2009,** *42* (14), 5226-5235.

23. Chambon, P.; Blanazs, A.; Battaglia, G.; Armes, S. P., Facile Synthesis of Methacrylic ABC Triblock Copolymer Vesicles by RAFT Aqueous Dispersion Polymerization. *Macromolecules* **2012,** *45* (12), 5081-5090.

24. Thompson, K. L.; Mable, C. J.; Cockram, A.; Warren, N. J.; Cunningham, V. J.; Jones, E. R.; Verber, R.; Armes, S. P., Are block copolymer worms more effective Pickering emulsifiers than block copolymer spheres? *Soft Matter* **2014,** *10* (43), 8615-8626.

25. Qu, Q. W.; Liu, G. Y.; Lv, X. Q.; Zhang, B. H.; An, Z. S., In Situ Cross-Linking of Vesicles in Polymerization-Induced Self Assembly. *Acs Macro Letters* **2016,** 5 (3), 316-320.

26. Zhang, L.; Lu, Q. Z.; Lv, X. Q.; Shen, L. L.; Zhang, B. H.; An, Z. S., In Situ Cross-Linking as a Platform for the Synthesis of Triblock Copolymer Vesicles with Diverse Surface Chemistry and Enhanced Stability via RAFT Dispersion Polymerization. *Macromolecules* **2017,** 50 (5), 2165-2174.

27. Zhou, W.; Qu, Q. W.; Yu, W. J.; An, Z. S., Single Monomer for Multiple Tasks: Polymerization Induced Self-Assembly, Functionalization and Cross-Linking, and Nanoparticle Loading. *Acs Macro Letters* **2014,** *3* (12), 1220-1224.

28. Stuart, M. A. C.; Huck, W. T. S.; Genzer, J.; Muller, M.; Ober, C.; Stamm, M.; Sukhorukov, G. B.; Szleifer, I.; Tsukruk, V. V.; Urban, M.; Winnik, F.; Zauscher, S.; Luzinov, I.; Minko, S., Emerging applications of stimuli-responsive polymer materials. *Nat. Mater.* **2010,** *9* (2), 101-113.

29. Tucker, B. S.; Sumerlin, B. S., Poly(N-(2-hydroxypropyl) methacrylamide)-based nanotherapeutics. *Polym. Chem.* **2014,** 5 (5), 1566-1572.

30. Pressly, E. D.; Rossin, R.; Hagooly, A.; Fukukawa, K. I.; Messmore, B. W.; Welch, M. J.; Wooley, K. L.; Lamm, M. S.; Hule, R. A.; Pochan, D. J.; Hawker, C. J., Structural effects on the biodistribution and positron emission tomography (PET) imaging of well-defined Cu-64-labeled nanoparticles comprised

of amphiphilic block graft copolymers. *Biomacromolecules* **2007,** *8* (10), 3126-3134.

31. Truong, N. P.; Whittaker, M. R.; Anastasaki, A.; Haddleton, D. M.; Quinn, J. F.; Davis, T. P., Facile production of nanoaggregates with tuneable morphologies from thermoresponsive P(DEGMA-co-HPMA). *Polym. Chem.* **2016,** *7*, 430-440.

32. Yang, J. Y.; Kopecek, J., Design of smart HPMA copolymer-based nanomedicines. *J. Controlled Release* **2016,** *240*, 9-23.

33. Ward, M. A.; Georgiou, T. K., Thermoresponsive triblock copolymers based on methacrylate monomers: effect of molecular weight and composition. *Soft Matter* **2012,** *8* (9), 2737-2745.

34. Truong, N. P.; Jia, Z. F.; Burgess, M.; Payne, L.; McMillan, N. A. J.; Monteiro, M. J., Self-Catalyzed Degradable Cationic Polymer for Release of DNA. *Biomacromolecules* **2011,** *12* (10), 3540-3548.

35. Fielding, L. A.; Lane, J. A.; Derry, M. J.; Mykhaylyk, O. O.; Armes, S. P., Thermo-responsive Diblock Copolymer Worm Gels in Non-polar Solvents. *J. Am. Chem. Soc.* **2014,** *136* (15), 5790-5798.

36. Blanazs, A.; Verber, R.; Mykhaylyk, O. O.; Ryan, A. J.; Heath, J. Z.; Douglas, C. W. I.; Armes, S. P., Sterilizable Gels from Thermoresponsive Block Copolymer Worms. *J. Am. Chem. Soc.* **2012,** *134* (23), 9741-9748.

37. Israelachvili, J. N.; Mitchell, D. J.; Ninham, B. W., Theory of Self-Assembly of Hydrocarbon Amphiphiles into Micelles and Bilayers. *J. Chem. Soc., Faraday Trans. 2* **1976,** *72*, 1525-1568.

38. Chen, J. Q.; Gong, X. L.; Yang, H.; Yao, Y. F.; Xu, M.; Chen, Q.; Cheng, R. S., NMR Study on the Effects of Sodium n-Dodecyl Sulfate on the Coil-to-Globule Transition of Poly(N-isopropylacrylamide) in Aqueous Solutions. *Macromolecules* **2011,** *44* (15), 6227-6231.

39. Zhang, C.; Peng, H.; Puttick, S.; Reid, J.; Bemardi, S.; Searles, D. J.; Whittaker, A. K., Conformation of Hydrophobically Modified Thermoresponsive Poly(OEGMA-co-TFEA) across the LCST Revealed by NMR and Molecular Dynamics Studies. *Macromolecules* **2015,** *48* (10), 3310-3317.

40. Zhang, C.; Moonshi, S. S.; Peng, H.; Puttick, S.; Reid, J.; Bernardi, S.; Searles, D. J.; Whittaker, A. K., Ion-Responsive F-19 MRI Contrast Agents for the Detection of Cancer Cells. *Acs Sensors* **2016,** *1* (6), 757-765.

41. Zhang, C.; Peng, H.; Li, W.; Liu, L. X.; Puttick, S.; Reid, J.; Bernardi, S.; Searles, D. J.; Zhang, A. F.; Whittaker, A. K., Conformation Transitions of Thermoresponsive Dendronized Polymers across the Lower Critical Solution Temperature. *Macromolecules* **2016,** *49* (3), 900-908.

42. Danial, M.; Tran, C. M. N.; Young, P. G.; Perrier, S.; Jolliffe, K. A., Janus cyclic peptide-polymer nanotubes. *Nat. Commun.* **2013,** *4*, 2780.

43. Stejskal, E. O.; Tanner, J. E., Spin Diffusion Measurements: Spin Echoes in the Presence of a Time-Dependent Field Gradient. *J. Chem. Phys.* **1965,** *42* (1), 288-+.

44. Ray, S. S.; Rajamohanan, P. R.; Badiger, M. V.; Devotta, I.; Ganapathy, S.; Mashelkar, R. A., Self-diffusion of water in thermoreversible gels near volume transition: Model development and PFG NMR investigation. *Chem. Eng. Sci.* **1998,** *53* (5), 869-877.

45. Deaton, K. R.; Feyen, E. A.; Nkulabi, H. J.; Morris, K. F., Pulsed-field gradient NMR study of sodium dodecyl sulfate micelle-peptide association. *Magn. Reson. Chem.* **2001,** *39* (5), 276-282.

46. Xu, J.; Mueller, R.; Hazelbaker, E.; Zhao, Y.; Bonzongo, J. C. J.; Clar, J. G.; Vasenkov, S.; Ziegler, K. J., Strongly Bound Sodium Dodecyl Sulfate Surrounding Single-Wall Carbon Nanotubes. *Langmuir* **2017,** *33* (20), 5006-5014.